J. Fluid Mech. (2003), *vol.* 477, *pp.* 1–18. © 2003 Cambridge University Press
DOI: 10.1017/S0022112002003129 Printed in the United Kingdom

Radial flow of two immiscible fluids: analytical solutions and bifurcations

By VAKHTANG PUTKARADZE

Department of Mathematics and Statistics, University of New Mexico, Albuquerque, NM 87131-1141, USA
putkarad@math.unm.edu

(Received 2 July 2001 and in revised form 28 August 2002)

We derive a novel set of analytical solutions of the Navier–Stokes equations describing stationary plane motion of two immiscible fluids emitted from a two-dimensional point source. The solutions are two-fluid generalizations of Jeffery–Hamel flows. The presence of an interface yields an unexpectedly rich and complex structure of solutions. Each set of physical parameter values admits a hierarchy of three different types of solution. The solutions bifurcate when parameters of the flow change sufficiently, with each type of solution having a different bifurcation diagram.

1. Introduction

Analytical solutions of the Navier–Stokes equations are ubiquitous in fluid mechanics. This paper is devoted to the derivation of a novel analytical solution of the Navier–Stokes equations involving the flow of two different fluids from a point source in a plane. The main motivation for this work is the extension of flows of Jeffery–Hamel type to the case of two immiscible fluids. The physical picture is the following: consider a two-dimensional source of one fluid being injected into another ambient fluid. Such flow may be realized for leakage from a cracked oil pipe submerged in water. We shall consider a slightly more general case: two viscous, incompressible fluids being ejected from the same point source in a plane. The setup of the flow is illustrated on figure 1. The two fluids are assumed immiscible and are separated by an interface, which is denoted by the two straight dashed lines originating at the source. We assume that fluid j, $j = 1, 2$, is flowing with the flow rate Q_j and has density ρ_j and kinematic viscosity ν_j. We emphasize that throughout this paper the effect of gravity is neglected.

The only case relevant for practical applications is $Q_1 \neq 0$, $Q_2 = 0$. We have found, however, that arbitrary $Q_2 \neq 0$ can be considered without extra effort. Thus, in the rest of the paper we shall consider arbitrary values of Q_1 and Q_2, although the case with $Q_2 \neq 0$ may be difficult to realize experimentally.

It is important to note that so far the experimental realization of these flows has eluded us (J. Deshler, V. Putkardze & P. Vorobieff, personal communicaton). However, we still believe that the two-fluid radial solutions are of interest because of the fundamental nature of idealized exact solutions of the Navier–Stokes equations. Since the interface between the fluids is assumed flat, the solutions remain valid for arbitrary values of surface tension (although the surface tension may introduce an instability to the flow). Thus, our idealized flows can also be useful for checking the results of numerical codes describing the motion of two fluids separated by an interface.

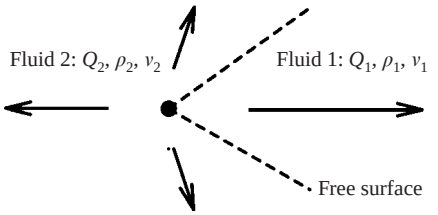

FIGURE 1. Diagram of the problem: two immiscible fluids being ejected from the same point source. The position of the free surface separating the two fluids is denoted by two dashed lines. We chose the polar coordinate system (r, ϕ) so that the source is at $r = 0$, the lower dashed line is $\phi = -\alpha/2$ and the upper dashed line is $\phi = \alpha/2$.

The flows developed in this paper are based on the classical Jeffery–Hamel solutions, which describe the outflow and inflow of viscous incompressible fluid in a linearly expanding channel (wedge) with a given angle between the solid walls as formulated by Jeffery (1915) and Hamel (1916). One dimensionless parameter of the problem is $R = Q/\nu$, Q being total flux and ν the kinematic viscosity, and another is the angle of the aperture, α. The behaviour of the solutions is very interesting. It was shown by Rosenhead (1940) that there is an infinity of solutions and each solution undergoes a bifurcation at some $R = R_c$, where the critical Reynolds number R_c depends on the number of oscillations in the velocity profile of the solution and the angle of the wedge. In spite of a long history, many important results illuminating the structure of Jeffery–Hamel solutions and their stability are very recent, see Fraenkel (1962), Eagles (1966), Moffatt & Duffy (1980), Eagles & Georgiou (1987), Georgion & Eagles (1988), Banks, Drazin & Zaturska (1988). Goldshtik & Shtern (1989), Goldshtik, Hussain & Shtern (1991), Dennis *et al.* (1997), Uribe *et al.* (1997).

There have been several generalizations of Jeffery–Hamel flows. An extension describing the flow of fluid in free space without boundaries was first considered in Berker (1963) but the analysis was not complete. Goldshtik & Shtern (1989) were the first to give the exact bifurcation values: it was shown that there is an infinity of solutions with k-fold symmetry, $k = 1, 2, \ldots$, and each such solution exists if $R \leqslant \pi(k^2 - 4)$. This type of flow was subsequently analysed in Goldshtik *et al.* (1991). Unaware of that earlier work, Putkaradze & Dimon (2000) re-derived the same results using analytic structure of solutions. Another generalization of Jeffery–Hamel solutions which includes a vortex and a sink at the origin was first made by Goldshtik *et al.* (1991). Voropayev and co-authors extended Jeffery–Hamel flows to include a quadrupole at the origin, see Voropayev & Afanasyev (1992, 1994), Voropayev, Fernando & Wu (1996) and Voropayev & Fernando (1996). Bourgin & Tahiri (1995) studied Jeffery–Hamel-type flows for the case when velocities on the interface are specified. Moffatt & Duffy (1980) posed different boundary conditions at the surface of the wedge and solved Jeffery–Hamel flow in the limit of small Reynolds numbers. Jeffery–Hamel flows were also used as a basis for the study of fluid flows in channels with curved walls by Fraenkel (1963) and Sobey & Drazin (1986).

The paper is structured as follows. First, we describe all possible types of solutions in § 2. An analysis of different types of stationary solutions is given in § 3. In § 4 we discuss the simplification of solutions for the case when only one fluid is present. Section 5 deals with overlapping regions of existence for different solutions in the parameter space. Finally, in § 6 we provide a conjecture on the possible number of solutions for given parameter values and briefly discuss the linear stability of solutions.

2. Different solutions: derivation

2.1. *Equations and boundary conditions*

The derivation of the governing equations in this paper is similar to that for Jeffery–Hamel flows. We shall therefore only go through the derivation briefly. For details, see Landau & Lifshitz (1987).

We assume that two immiscible, incompressible fluids are ejected from a point source in two dimensions, as illustrated on figure 1. The fluids have kinematic viscosities ν_1 and ν_2 and densities ρ_1 and ρ_2. If we assume that the fluids are flowing purely radially, i.e. $v_\phi = 0$ in each, the incompressibility condition $\partial_r(r v_r) = 0$ gives

$$v_{r,j} = \nu_j \frac{u_j(\phi)}{r}. \tag{2.1}$$

Here and below, the subscript $j = 1, 2$ indexes the fluid. The prefactor ν_j in (2.1) makes the velocity function $u_j(\phi)$ dimensionless. For convenience, substitute

$$u_j(\phi) = -6 f_j(\phi) - 2, \tag{2.2}$$

then each of the functions $f_j(\phi)$ satisfies a single ordinary differential equation:

$$f_j'^2 = 4 f_j^3 - a_j f_j - b_j, \tag{2.3}$$

where the constants a_j and b_j, $j = 1, 2$, are to be determined to satisfy boundary conditions at the interfaces. The prime denotes the derivative with respect to ϕ. We assume that the interface is located at $\phi = -\alpha/2$ and $\phi = \alpha/2$. If we denote the viscosity ratio $\lambda = \nu_1/\nu_2$ and define $\delta = \lambda^2 \rho_1/\rho_2$, the boundary conditions at the interface become

$$\lambda(6 f_1(-\alpha/2) + 2) = 6 f_2(-\alpha/2) + 2, \quad \lambda(6 f_1(\alpha/2) + 2) = 6 f_2(\alpha/2) + 2, \tag{2.4a}$$

$$\delta f_1'(-\alpha/2) = f_2'(-\alpha/2), \quad \delta f_1'(\alpha/2) = f_2'(\alpha/2), \tag{2.4b}$$

$$\delta(3a_1 - 4) = 3a_2 - 4, \tag{2.4c}$$

$$\int_{-\alpha/2}^{\alpha/2} (-6 f_1(\phi) - 2)\, \mathrm{d}\phi = R_1, \quad \int_{\alpha/2}^{2\pi-\alpha/2} (-6 f_2(\phi) - 2)\, \mathrm{d}\phi = R_2. \tag{2.4d}$$

Here, (2.4*a*) is the continuity of velocity across the interface, (2.4*b*) is the continuity of tangential stress and (2.4*c*) is the continuity of normal stress. Finally, (2.4*b*) is the flux condition for each fluid with corresponding Reynolds numbers defined as $R_j = Q_j/\nu_j$.

Boundary conditions (2.4) yield seven equations, since the normal stress tensor (2.4*c*) is constant throughout the fluid. There are also seven unknowns: a_j, b_j, $j = 1, 2$ and initial conditions for (2.3), together with the angle occupied by the first fluid α. The solutions of the differential-algebraic problem (2.3) and (2.4) can be found by Newton iterations starting with $\lambda = \delta = 1$, corresponding to the flow of a single fluid from a point source, described in detail in Goldshtik *et al.* (1991). Choosing a solution with a certain periodicity m, we continue it towards the desired values of parameters λ and δ. To start the continuation, we need to choose the position of the 'interface' at $\phi = -\alpha_0/2$ and $\phi = \alpha_0/2$. We found that the choice strongly depends on the values of α_0 and the chosen initial profile, showing that several solutions of this problem are possible. In the remainder of the paper, we present an alternative method of studying the solutions. The method allows the complete classification of the hierarchy of solutions, and also yields solutions which are impossible to obtain by

Newton's method with continuation (SE solutions, see below). Our method consists of finding the solutions satisfying the boundary conditions at $\phi = \alpha/2$ automatically provided they satisfy the boundary conditions at $\phi = -\alpha/2$. For these specific types of solutions, the problem becomes analytically tractable. Note that these are the only solutions we were able to find numerically.

The classification of solutions is achieved using the theory of Weierstrass Elliptic Functions (P-functions). Unfortunately, we could not find a satisfactory explanation of our method without using the P-functions, but we shall try to keep the technical details to a minimum. The only property of elliptic functions we shall use is the double-periodicity in the complex plane. To make the paper self-contained, we start the following subsection with the explanation of the double-periodicity of P-functions. This will also allow us to introduce some useful notation.

2.2. *Analytic properties of the solutions*

Equation (2.3) can be interpreted as a description of the motion of a particle in a cubic potential $U(f) = -4f^3 + a_j f + b_j$, which shows that the solutions of (2.3) are periodic with some period, let us say p_j, with p_j being real. Upon the change of variables $\phi \to \mathrm{i}\phi$, equation (2.3) describes motion of a particle in a cubic potential $-U(f)$, which shows that the solution $f_j(\phi)$ is periodic with imaginary period $2\mathrm{i}\tau_j$. In other words, we necessarily have $f_j(\phi + p_j) = f_j(\phi + 2\mathrm{i}\tau_j) = f_j(\phi)$. This is a consequence of the more general fact that solutions of (2.3) – Weierstrass Elliptic Functions – are doubly periodic functions in the complex plane, see, for example, Chandrasecharan (1984). Periods are connected to the invariants through the formulas

$$\left.\begin{aligned} a_j &= 60{\sum_{n,m}}'(np_j + m2\mathrm{i}\tau_j)^{-4}, \\ b_j &= 140{\sum_{n,m}}'(np_j + m2\mathrm{i}\tau_j)^{-6}, \end{aligned}\right\} \tag{2.5}$$

where the prime denotes that the summation is taken over all integers n, m such that n and m are not both zero. In general, the periods may be two arbitrary linearly independent complex numbers.

The solution of (2.3) can be represented either in terms of invariants, i.e. a_j and b_j, or in terms of periods, i.e. p_j, $2\mathrm{i}\tau_j$. These representations are completely equivalent from the mathematical point of view. Depending on the case, however, it is advantageous to use either the invariants or the periods representation. To distinguish between these representations, we shall denote $f(z) = \mathscr{P}(z; a_j, b_j)$ if $f(z)$ is represented in terms of invariants a_j and b_j, and use curly brackets after the semicolon $f(z) = \mathscr{P}(z; \{p_j, 2\mathrm{i}\tau_j\})$ if $f(z)$ is represented in terms of periods $p_j, 2\mathrm{i}\tau_j$. Also, we always explicitly mention which representation is used in each particular case to avoid confusion.

2.3. *Satisfying boundary conditions at $\phi = -\alpha/2$ and $\phi = \alpha/2$*

We are now ready to describe different types of solutions obeying boundary conditions (2.4). As was mentioned earlier, we seek solutions satisfying boundary conditions at $\phi = \alpha/2$ provided that boundary conditions at $\phi = -\alpha/2$ are satisfied.

The first possibility is to seek solutions $f_1(\phi)$, which are periodic with the real period $p_1 = \alpha/k_1$, and $f_2(\phi)$ with the real period $p_2 = (2\pi - \alpha)/k_2$ for some integer numbers k_1 and k_2. Using our mechanical analogy, solutions of this type represent a particle oscillating in a cubic potential $U(f) = -4f^3 + a_j f + b_j$. For each fluid,

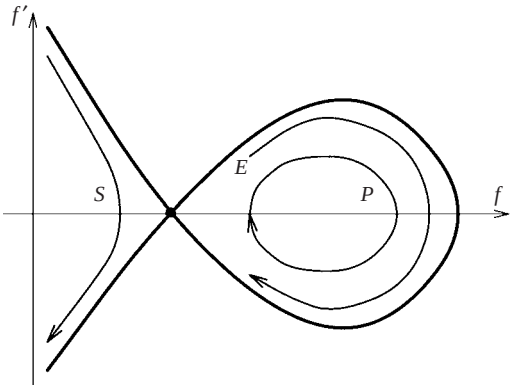

FIGURE 2. Three different types of solutions on the (f, f') phase plane.

such solutions correspond to a closed trajectory on the (f, f') phase plane, marked with the letter P on figure 2. We distinguish different periodic solutions by their periodicity. We denote solutions with $f_1(\phi)$ being k_1 periodic and $f_2(\phi)$ being k_2 periodic as $P(k_1)P(k_2)$ (periodic–periodic). In the analysis of $P(k_1)P(k_2)$ solutions we will use the period representation. The $P(k_1)P(k_2)$ solutions are given by

$$f_j(\phi) = \mathscr{P}(\phi + \mathrm{i}\tau_j + \theta_j, \{p_j, 2\mathrm{i}\tau_j\}). \tag{2.6}$$

The unknowns are θ_j (phase shifts) and τ_j (imaginary periods).

The second possibility is to require the flow to be symmetric with respect to reflection about the line $\phi = 0$, more precisely $f_1(-\phi) = f_1(\phi)$, $f_2(\pi - \phi) = f_2(\pi + \phi)$. An example of a solution of this type is marked on figure 2 with the letter E. In schematic figure 2, the period of the E solution is larger than the period of P. Since there is no condition on the periods, the representation of solutions in terms of invariants a_j, b_j is advantageous. Solutions of this kind are given by:

$$\left.\begin{aligned} f_1(\phi) &= \mathscr{P}(\phi + \mathrm{i}\tau_1(a_1, b_1); a_1, b_1), \\ f_2(\phi) &= \mathscr{P}(\pi + \phi + \mathrm{i}\tau_2(a_2, b_2); a_2, b_2). \end{aligned}\right\} \tag{2.7}$$

The unknowns are the invariants a_j and b_j. The imaginary half-periods $\tau_j(a_j, b_j)$ can be expressed in terms of the invariants (a_j, b_j) by inverting (2.5). Even though no requirements on real periods are made, we shall enumerate these solutions in terms of two integer numbers, k_1 and k_2. This implies that the real periods p_j satisfy

$$\left.\begin{aligned} \frac{\alpha}{k_1} \leqslant p_1 \leqslant \frac{\alpha}{k_1 + 1}, \\ \frac{2\pi - \alpha}{k_2} \leqslant p_2 \leqslant \frac{2\pi - \alpha}{k_2 + 1}. \end{aligned}\right\} \tag{2.8}$$

We shall denote such solutions $E(k_1)E(k_2)$ ('even–even'). Note that a P or E solution with infinite real period corresponds to a separatrix.

The third possibility is for one of the solutions $f_j(\phi)$ to be singular. From the properties of equation (2.3) we conclude that singularities of $f_j(\phi)$ are periodically spaced second-order poles: $f_j \sim (z - np_j)^{-2}$, where n is any integer number. These solutions are physical if the singularity occurs outside the domain of the solution, i.e. in another fluid. For example, if $f_1(\phi)$ is such singular solution, we need the singularities of $f_1(\phi)$ to lie outside the region $-\alpha/2 \leqslant \phi \leqslant \alpha/2$. In this case, $f_1(\phi)$

cannot be periodic, since that would necessarily mean having singularities inside the domain $-\alpha/2 \leqslant \phi \leqslant \alpha/2$. Thus, $f_1(\phi)$ must be a symmetric function of ϕ: $f_1(-\phi) = f_1(\phi)$. A solution of this type is marked on figure 2 with the letter S ('singular'). Then, $f_2(\phi)$ must be a symmetric function of ϕ also. From the boundary conditions one can deduce that $f_2(\phi)$ must be a non-singular symmetric function, i.e. of type $E(k_2)$. Therefore, the third type of solution is given by putting together a singular symmetric solution S and non-singular symmetric solution E. This can be done in two possible ways: $SE(k_2)$ ($f_1(\phi)$ being singular) and $E(k_1)S$ ($f_2(\phi)$ being singular). In what follows, we only consider $SE(k_2)$ solutions – the development for $E(k_1)S$ is completely analogous. For $SE(k_2)$ solutions, we use a representation in terms of invariants:

$$\left.\begin{aligned} f_1(\phi) &= \mathscr{P}(\phi; a_2, b_2), \\ f_2(\phi) &= \mathscr{P}(\pi + \phi + \mathrm{i}\tau_2(a_2, b_2); a_2, b_2). \end{aligned}\right\} \tag{2.9}$$

Again, the unknowns are a_j, b_j and α. We note that we have only observed singular solutions of the type illustrated on figure 2. It is possible that a singular solution enclosing a separatrix exists, but we have not observed it.

The fourth possibility is for one of the functions f_j to be constant, and another function oscillatory. One can see that if, for example, $f_2 = \text{const}$, $f_1(\phi)$ must be periodic with the period α/k_1. We shall call these solutions $P(k_1)C$ solutions if $f_2 = \text{const}$ and $CP(k_2)$ if $f_1 = \text{const}$.

Finally, the most trivial solution possible is the one with $f_1 = \text{const}$ and $f_2 = \text{const}$. We shall refer to these solutions as CC solutions.

As we shall see below, three cases $P(k_1)P(k_2)$, $E(k_1)E(k_2)$, $SE(k_2)$ are obtained for the set of parameters (R_1, R_2) of positive measure. Other types of solutions, involving at least one C in their notation, can only be obtained for sets of codimension at least one in the parameter space (R_1, R_2). Therefore, we concentrate on the analysis of the $P(k_1)P(k_2)$, $E(k_1)E(k_2)$ and $SE(k_2)$ types of solution as physically relevant. However, we shall mention $P(k_1)C$ and $CP(k_2)$ solutions later as they play an important role in bifurcations.

We shall now commence the detailed analysis of the solutions. All the formulas in the rest of the paper are derived for arbitrary fluxes, viscosities and densities of the fluids. All the examples are computed for viscosity ratio $\nu_1/\nu_2 = 0.5$ and density ratio $\rho_1/\rho_2 = 0.5$.

3. Structure of solutions

3.1. *Solutions of type* $P(k_1)P(k_2)$

All the formulas in the discussion of $P(k_1)P(k_2)$ solutions are derived for general k_1 and k_2. The computations are performed for $k_1 = 1, k_2 = 3$ as an example.

It is easiest to analyse the $P(k_1)P(k_2)$ case using the description of the solution in terms of complex periods. In this case, as we have mentioned before, $f_1(\phi)$ is periodic with periods $\{\alpha/k_1, 2\mathrm{i}\tau_1\}$ and $f_2(\phi)$ is periodic with periods $\{(2\pi - \alpha)/k_2, 2\mathrm{i}\tau_2\}$. The solution for $f_j(\phi)$ is given by (2.6). The five unknown quantities α, τ_j, θ_j must be expressed in terms of R_1 and R_2. We have chosen an alternative approach: to parameterize the solutions by the angle α and one of the periods τ_1 or τ_2, rather than R_1 and R_2. This reduces the number of unknowns to three and R_1, R_2 are then computed from (2.4*d*). The detailed algorithm for finding solutions is presented in Appendix A. The rest of this section is devoted to the study of the bifurcation structure of $P(1)P(3)$ solutions.

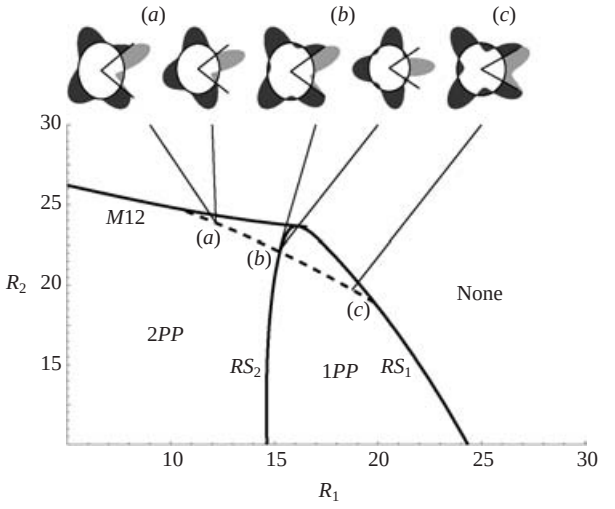

FIGURE 3. Domain of existence of the solutions of type $P(k_1)P(k_2)$ with $k_1 = 1$ and $k_2 = 3$. Diagrams at the top show velocity profiles, with parameter values for these solutions labelled (*a–c*). The diagrams show the velocity function $u(\phi)$ connected to the velocity through (2.1). The circle corresponds to the zero of $u_j(\phi)$, and radial deviation from the circle is proportional to $u(\phi)$. On the diagrams, the straight radial solid lines indicate position of the interface, and the light grey and dark grey shadings correspond to fluids 1 and 2 respectively. Thin solid lines pointing from diagrams to a point in the parameter space indicate for which values of parameters (R_1, R_2) the flows were computed. The value of the derivative of f_1' on the interface (proportional to the tangential component of the stress tensor) is computed along the dashed line. The regions where two, one and zero $P(1)P(3)$ solutions exist are marked $2PP$, $1PP$ and None, respectively. Bifurcation lines are labelled $M12$ (corresponding to Merging of two solutions) and RS_1, RS_2 (corresponding to a PP solution becoming Reflectionary Symmetric).

A $P(k_1)P(k_2)$ solution might cease to exist under one of the following conditions:

(i) one of the complex periods τ_j goes to $+\infty$;

(ii) a solution ceases to be real.

The first possibility would occur in the case when one of the solutions $f_j(\phi)$ approaches a constant, whereas another solution remains oscillatory. In our notation, such solutions are denoted $CP(k_2)$ or $P(k_1)C$. We have discovered, however, that although solutions with $f_1(\phi) = \text{const}$ and $f_2(\phi)$ oscillating (and vice versa) exist, they are isolated from the domain of existence of $P(k_1)P(k_2)$ solutions, at least for the case $k_1 = 1, k_2 = 3$. The bifurcations of the second type occur when two solutions merge for some parameter values. There are two possibilities. First, a solution can collide with its reflectionary-symmetric counterpart. We call these solutions $PE(k_1)PE(k_2)$, since they are both periodic and even. Bifurcations of this type are characterized by the vanishing derivative of f at the interface. Second, two different solutions (unrelated by reflectional symmetry) can merge. In this case, the value of the derivative at the interface need not go to zero.

We draw the domain of existence of the solutions and several examples on figure 3. The solid lines show the values of parameters (R_1, R_2) for which bifurcations of solutions occur. At most, two different solutions of this type are possible for given values of parameters (R_1, R_2), together with the reflection about $\phi = 0$ that gives four solutions. The domain where two different solutions are possible is therefore marked '$2PP$' on figure 3. The domain of existence of two different PP solutions is bounded by the lines marked RS_1, where one of the solutions collides with its

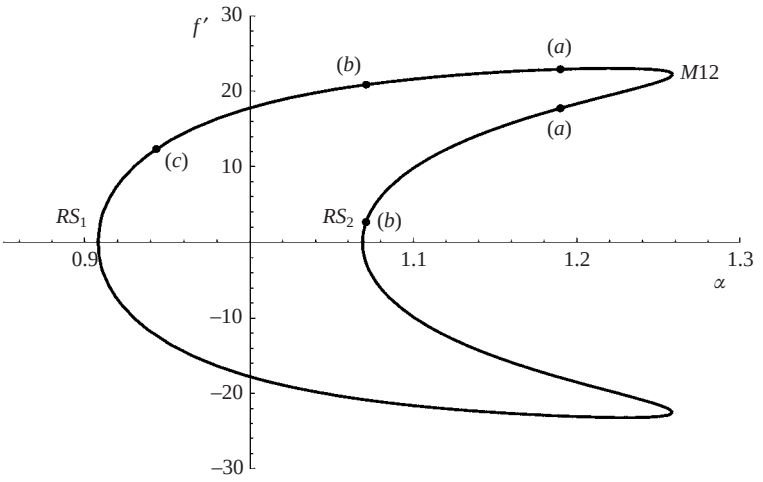

FIGURE 4. $f_1'(\alpha/2)$ along a curve in parameter space intersecting all bifurcation lines (dashed line on figure 3). The lower portion of the diagram represents the solution symmetrical with respect to reflection about $\phi = 0$. The folds correspond to the bifurcation lines on figure 3, which is emphasized by the labelling of the folds $M12$, RS_1, RS_2. Letters (a–c) indicate the positions of examples computed on figure 3.

reflectional-symmetric counterpart, and $M12$, denoting merging of the first and second solutions. The set of examples (a) is computed below the $M12$ line. Notice that the two (a) solutions are visually very close. Beyond the line RS_2, only one non-trivial $P(1)P(3)$ solution exists, another one being its reflectionary-symmetric image. The domain of existence of one $P(1)P(3)$ solution is marked $1PP$. This domain is bounded by the lines RS_1 on one side and RS_2 on the other. The line RS_1 marks the values of parameters where the last remaining solution achieves reflectional symmetry and thus collides with its reflectionary-symmetric image. No solution exists anywhere else, which is marked 'None' on figure 3. Examples (b) are computed for parameter values to the left of the RS_2 line, and example (c) is computed to the left of the RS_1 line. Because of the closeness to the corresponding bifurcation lines, one of the solutions of set (b) and solution (c) are close to being reflectionary-symmetric. Notice that all the bifurcation lines in the parameter plane intersect at one point with continuous slopes.

We shall now briefly explain the notation for velocity profiles at the top of figure 3. The velocity in the fluid is shown as the filled curve: one of the boundaries is given by the circle with the radius r_0 corresponding to zero velocity. The other boundary of the filled curve is given by $u_0 + u(\phi)$, where $u(\phi)$ is the velocity function defined by (2.1) and (2.2). We remind the reader that $u(\phi)$ is dimensionless and $v_{r,j} = v_j u_j(\phi)/r$ according to (2.1). The radius u_0 corresponding to the zero of the velocity function was chosen to be 15. The light grey colour corresponds to the first fluid, and the dark grey colour to the second fluid.

To investigate further, we computed $f_1'(\alpha/2)$ along the dashed line on figure 3. This line can be parameterized by the angle occupied by the first fluid α. The results of our calculations are shown on figure 4. The solid dots with labels show the values corresponding to the examples on figure 3. Three fold bifurcations are observed: one at $\alpha \simeq 0.905$ corresponding to line RS_1 on figure 3, one at $\alpha \simeq 1.07$ corresponding to the crossing of line RS_2 and one at $\alpha \simeq 1.26$ corresponding to line $M12$. The

bifurcation diagram for solutions of type $P(k_1)P(k_2)$ is typical for catastrophes of corank two. The point of intersection of lines $M12$, RS_1, RS_2 defines a point of double degeneracy in the space of parameters R_1 and R_2. Since a $P(k_1)P(k_2)$ solution reflected with respect to the line $\phi = 0$ is also a solution, there is an additional requirement of symmetry. This structure of the catastrophe can be understood by analysing the solutions close to the point of double degeneracy. It is interesting that the catastrophe structure is equivalent to the hyperbolic umbilic not only locally, but also globally. For more details on this type of catastrophe we refer the reader to Thom (1975).

3.2. *Solutions of type* $E(k_1)E(k_2)$

Since there is no condition on the period of the $E(k_1)E(k_2)$ solutions, it is more convenient to use the parameterization of solutions in terms of the invariants a_j, b_j. Thus, we take a_j, b_j and the angle α to be the unknowns. The algorithm for finding solutions is quite similar to that of $P(k_1)P(k_2)$ solutions and we shall only discuss it briefly.

One of the variables, say a_1, can be eliminated using (2.4*c*). Analogously to the discussion of $P(k_1)P(k_2)$ solutions, the values of f_1 and f_2 at the interface can be computed in terms of a_j and b_j from (A 3) in the Appendix. Putting $\phi = -\alpha/2$ in (2.7) yields two equations:

$$\left.\begin{aligned} f_1 &= \mathscr{P}(-\alpha/2 + \mathrm{i}\tau_1(a_1, b_1); a_1, b_1), \\ f_2 &= \mathscr{P}((2\pi - \alpha)/2 + \mathrm{i}\tau_2(a_2, b_2); a_2, b_2). \end{aligned}\right\} \tag{3.1}$$

Two more unknowns can be eliminated using (3.1) provided that each f_j satisfies $f_{j,min} \leqslant f_j \leqslant f_{j,max}$, where $f_{j,min/max}$ are defined in the Appendix. Finally, two more variables are eliminated through the flux conditions (2.4*d*).

Loss of solutions may occur if one of the roots of (A 3), f_j, reaches either $f_{j,min}$ or $f_{j,max}$. At this point, the derivative of the solution f at the interface becomes zero. Thus, at the point of bifurcation, solutions $f_1(\phi)$ and $f_2(\phi)$ are either constants or have an integer number of periods fitting in α and $2\pi - \alpha$, respectively. Such solutions form the boundaries of the areas of existence of $E(k_1)E(k_2)$ solutions. We present the domain of existence of $E(1)E(1)$ solutions on figure 5 as an example. We found that $E(1)E(1)$ solutions can bifurcate in two possible ways:

(*a*) the solution for fluid 1 attains the period α and the solution for fluid 2 approaches a constant (line P_1C on figure 5, corresponding to $P(1)C$ solutions);

(*b*) the solutions for fluid 1 and fluid 2 become periodic with the periods α and $2\pi - \alpha$, respectively (line PE_1PE_1 on figure 5, corresponding to the reflectionary symmetric $P(1)P(1)$ solutions, or $PE(1)PE(1)$ in our notation).

The curves P_1C and PE_1PE_1 intersect at the origin with discontinuous slopes. On both curves, the derivative of the function $f_j(\phi)$ at the interface becomes zero. This is illustrated by two examples of EE solutions on figure 5. The example to the left is taken on the boundary PE_1PE_1 which is manifested in the solution being periodic in each fluid. The example to the right, on the other hand, is on the curve P_1C, and therefore the velocity in the second fluid is constant. Across the bifurcation lines, solutions merge with other EE solutions through a fold bifurcation, which is common for the flows of Jeffery–Hamel type. A similar bifurcation structure seems to be realized for other values of k_1 and k_2.

3.3. *Solutions of type* $SE(k_2)$

The method for calculating $SE(k_2)$ solutions is very similar to that for $E(k_1)E(k_2)$ described above. Again, we take a_j, b_j and α as unknowns. One of the unknowns can

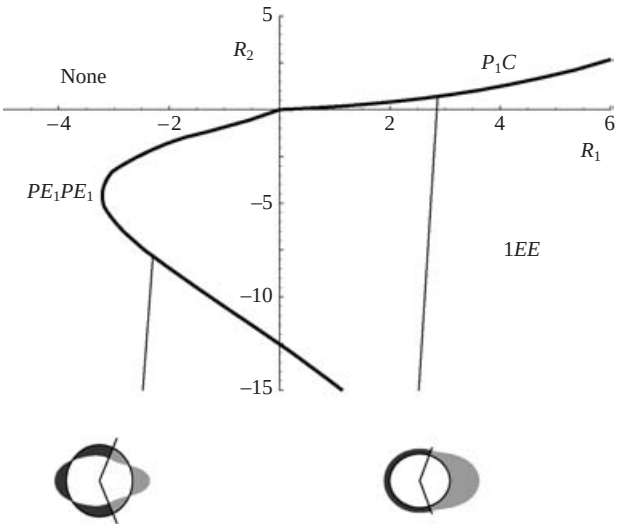

FIGURE 5. Domain of existence of solutions of the EE type with $k_1 = 1, k_2 = 1$. Several examples of solutions are also shown. Labels $1EE$ and None mark the regions with one and no $E(1)E(1)$ solutions, respectively. P_1C and PE_1PE_1 label the type of bifurcation. Two examples of the solutions are shown.

be eliminated using (2.4c). Given a_j, b_j, we can find the values of $f_{1,2}$ at the interface using (A 3) in the Appendix. The values of $f_{1,2}$ give rise to equations at the interface

$$\left.\begin{aligned} f_1 &= \mathscr{P}(\alpha/2; a_1, b_1), \\ f_2 &= \mathscr{P}((2\pi - \alpha)/2 + \mathrm{i}\tau_2(a_2, b_2); a_2, b_2). \end{aligned}\right\} \tag{3.2}$$

Notice the difference between the first equation of (3.1) and (3.2). We can now eliminate two unknowns from (3.2); this brings the number of unknowns to two. Finally, the last two unknowns can be eliminated using the flux conditions (2.4d).

Even though the method for obtaining $SE(k_2)$ flows is very similar to that for $E(k_1)E(k_2)$ flows, the bifurcation structure is different. Indeed, the function $f_1(\phi)$ given by the first equation of (2.9) only has zero derivative at $\phi = 0$, thus it is impossible for the bifurcation through $f_1'(\phi)$ to be zero at the interface. Our studies have shown that the $SE(1)$ solution bifurcates in one of the following ways:

(a) The imaginary period of $f_1(\phi)$ approaches infinity corresponding to $a_1^3 - 27b_1^2 = 0$ (line 'Infinite τ' on figure 6). Very close to the line on figure 6,

$$f_1(\phi) \simeq \frac{1}{\cos^2 \pi\phi/p_1},$$

where p_1 is the real period of $f_1(\phi)$. On the infinite τ line, the $SE(1)$ solution merges with another $SE(1)$ solution which has a complex set of periods in the first fluid (S) forming a parallellogram rather than a rectangle (meaning that it is no longer possible to separate periods of the elliptic function into purely real and imaginary, as they both are complex).

(b) Gradients of velocity at the interface reach maximum value (line 'Max Grad'– maximum gradients – on figure 6). According to (2.3), the maximum allowable value

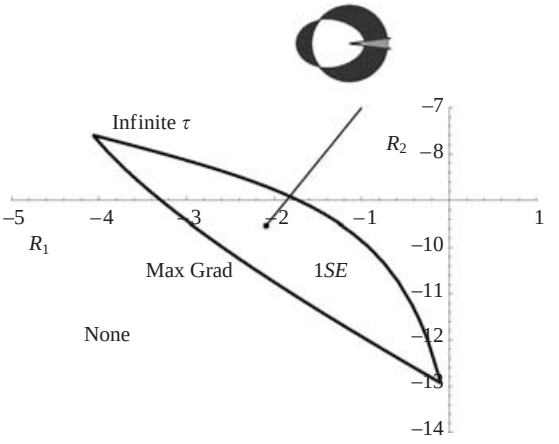

FIGURE 6. Domain of existence of solutions of the $SE(k_2)$ type with $k_2 = 1$. Labels $1SE$ and None mark the regions with one and no $SE(1)$ solutions, respectively. An example of the solutions is shown.

of the derivative is achieved when $f'' = 0$ and is given by

$$f'^2_{j,max} = \pm\frac{a_j^{3/2}}{3\sqrt{3}} - b_j.$$

The solution cannot exist if the value of the derivative at the surface is required to be larger than $f'_{j,max}$. On the Max Grad line, the solution also merges with another $SE(1)$ solution of the type similar to one arising at the infinite τ line.

It is interesting to note that solutions of the type $SE(1)$ exist only for a finite range of (R_1, R_2) in the area bounded by the lines Infinite τ and Max Grad on figure 6. Since the outflow–inflow diagrams for SE solutions are visually very similar throughout the existence domain, we have chosen to only show one example in the middle of the existence domain on figure 6. From this example, we see that for $SE(1)$ solutions the angle α tends to be very small.

We now explain why SE or ES solutions are impossible to obtain by continuation of single-fluid solutions from $\lambda = \delta = 1$. Indeed, suppose such continuation were possible for an SE solution, for example. At $\lambda = \delta = 1$, the fluids become identical and there is no interface any more, so the flow in the second fluid is the analytic continuation of the flow in the first fluid. But we know that the solution of the first fluid, continued analytically in the domain of the other fluid, exhibits singularities in the form of second-order poles. Thus, the limiting solution for $\lambda = \delta = 1$ must have poles, which is impossible.

4. The case when the first fluid is inviscid

In this section, we show how to compute solutions in the simplified case when the first fluid is inviscid, implying $\lambda = \delta = 0$. We note that the question of the limiting behaviour $\lambda \to 0$ is difficult and falls beyond the scope of this article.† In this case, the

† Recently, the case of two fluids flowing from a source with $\lambda \ll 1$ was considered by professors P. Weidman and A. Herczynski (private communication). Their solution, obtained by the boundary layer approach, does not satisfy the assumption of radial flow. This work confirms the extremely delicate nature of the limit $\lambda \to 0$.

boundary conditions for the second fluid separate from the motion of first fluid and are identical to the boundary conditions at a free surface, as we shall see immediately below. The motion of a viscous fluid can be computed independently of the motion of an inviscid fluid. (We remind the reader that the gravity effects have been neglected.) Therefore, such solutions will also describe a fluid shooting out of a long crack in the side of a pipe into air. Since we are interested only in the motion of one (viscous) fluid, we shall call these flows *single-fluid solutions*. We shall see, however, that single-fluid solutions occur only for $R < 0$, which corresponds to radial inflow. It is hard to imagine an experiment of this sort, but we present the solutions nevertheless for the sake of completeness. Since we are only interested in computing the flow of one fluid, everywhere in this section we drop the subscript labelling the fluid. There are no boundary conditions on the radial velocity. Thus, boundary conditions (2.4) simplify to

$$f'(-\alpha/2) = 0, \quad f'(\alpha/2) = 0, \tag{4.1a}$$

$$a = 4/3, \tag{4.1b}$$

$$\int_{-\alpha/2}^{\alpha/2} (-6f(\phi) - 2)\,\mathrm{d}\phi = R, \tag{4.1c}$$

and $f(\phi)$ satisfies (2.3). Since the derivatives of the function $f(\phi)$ are zero at the boundaries and $f(\phi)$ is non-singular, solutions of the type S are impossible. Hence, $f(\phi)$ is given by

$$f(\phi) = \mathscr{P}(\phi + \mathrm{i}\tau + \theta, \{p, 2\mathrm{i}\tau\}). \tag{4.2}$$

In (4.2), we use the period representation of the elliptic function. The unknowns are p, τ, θ, which have to be determined from the three equations (4.1). We shall now demonstrate the advantages of using Weierstrass Elliptic Functions by choosing the parameterization of solutions in such a way that the equations are satisfied automatically. Using the asymptotics of elliptic functions, we construct the approximate yet extremely accurate conditions for the existence of solutions.

Notice first that the derivative of $f(\phi)$ defined by (4.2) vanishes only at $\phi = mp$ or $\phi = (m + 1/2)p$, where m is any integer number. Therefore,

$$\left.\begin{array}{c} p = 2\alpha/k \\ \theta = 0 \quad \text{or} \quad \theta = p/2. \end{array}\right\} \tag{4.3}$$

In (4.3), k is an integer, with k being even corresponding to the solutions symmetric with respect to reflection about line $\phi = 0$. Next, define $\xi = \tau/p$ and use ξ as the parameter. From (2.5) and (4.3) we conclude that

$$p = \frac{2\alpha}{k} = \left(\tfrac{3}{4}a(1, 2\mathrm{i}\xi)\right)^{1/4}. \tag{4.4}$$

Again, the flux equation (4.1c) can be computed in terms of a Weierstrass Zeta Function ζ:

$$R(k, \xi) = \frac{6k^2}{\alpha}\zeta(1; \{2, 2\mathrm{i}\xi\}) - 2\alpha. \tag{4.5}$$

Given an integer number k and a real value of the parameter ξ, the angle α is determined from (4.4), which gives real period p, imaginary period $2\mathrm{i}\tau = 2\mathrm{i}\xi p$ and the solution (4.2). The dimensionless flux R is determined from (4.5). Bifurcations of solutions occur if α goes outside the range $(0, 2\pi)$ or if $\xi \to \infty$. In the second case, the velocity profile approaches a constant.

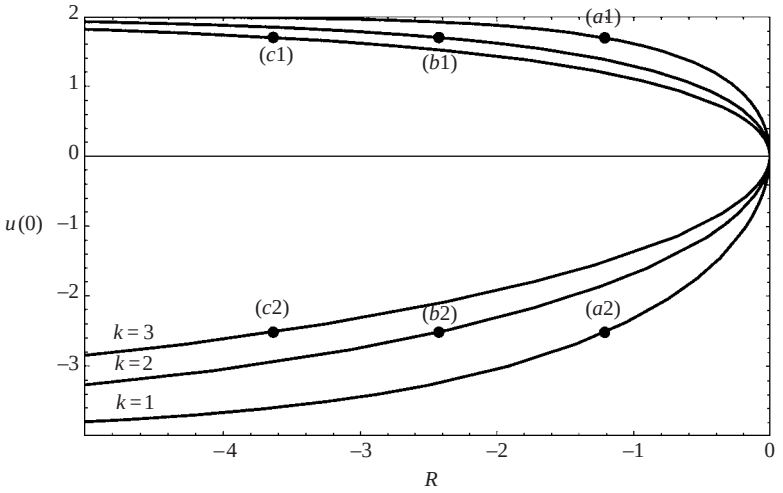

FIGURE 7. Bifurcations of the flow of a viscous fluid into inviscid fluid or air. Vertical coordinate is velocity on the interface $u = -6f - 2$ and horizontal coordinate is R. Labelled dots refer to figure 8.

The condition $0 < \alpha < 2\pi$ determines the number of physically permissible solutions. Using expressions (2.5), one can show that when $\xi \to \infty$, $a(1, 2i\xi) \to 4/3\pi^4$, so $\alpha \to \pi k/2$. Also, one can demonstrate that $a(1, 2i\xi)$ is a decreasing function of ξ. Therefore, there are at most three solutions with $k = 1, 2, 3$.

The condition $\alpha < 2\pi$ imposes the constraint $\xi > \xi_{k,*}$ for each k. The values of $\xi_{k,*}$ are very close to $k/8$, which can be shown by using the asymptotic expressions for $a(1, 2i\xi)$ for small ξ:

$$a(1, 2i\xi) \simeq \frac{\pi^4}{12\xi^4}(1 + \epsilon(\xi)), \tag{4.6}$$

where $\epsilon(\xi)$ is a function exponentially small in $1/\xi$. At the critical value of $\xi = \xi_{k,*}$ we have $\alpha(\xi) = 2\pi$. This condition together with (4.6) and (4.4) give $\xi_{k,*} \simeq k/8 +$(exponentially small terms in $1/\xi$). Numerically computed values of $\xi_{k,*}$ are: $\xi_{1,*} \simeq 0.1250000000912$, $\xi_{2,*} \simeq 0.2500524333087$, $\xi_{3,*} \simeq 0.3807524621457$.

The limit $\xi \to \infty$ of the Weierstrass Zeta Function in (4.5) can be computed analytically as well: $\zeta(1; 2, 2i\xi) \to \pi^2/12$. Since $\alpha(k, \xi) \to \pi k/2$, we have $R(k, \xi) \to 0$ when $\xi \to \infty$. Therefore, all the solutions are defined for $R \leqslant 0$.

On figure 7, we present the dependence of the velocity at the interface $u(0) = -6f(0) - 2$ on the parameter R. The upper lines correspond to the choice $\theta = 0$ and the lower lines to $\theta = p/2$. We see that $R = 0$ is the bifurcation point for all the solutions, and the bifurcation is of the fold type. We find this feature very interesting and unexpected, since in the classical Jeffery–Hamel flows and their generalizations the solutions with different numbers of wiggles bifurcate at different Reynolds numbers.

We also compute all possible flows for $\xi = 0.9$. The points where the flows are calculated are marked on figure 7 with solid dots labelled a, b, c. Velocity profiles are shown on figure 8, labelled accordingly. Each pair of profiles at the top ($k = 1$) and at the bottom ($k = 3$) of the picture is connected by reflection about $\phi = 0$. The profiles in the middle ($k = 2$) are symmetric with respect to reflection about $\phi = 0$.

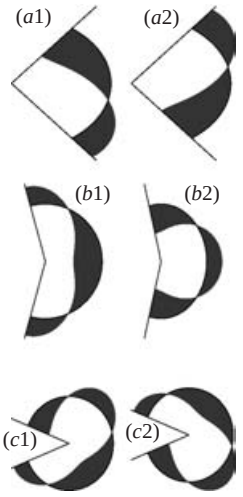

FIGURE 8. Examples of single-fluid flows. Top to bottom: $k = 1, 2, 3$. Left to right: $\theta = 0$ and $\theta = p/2$. The labels mark the position of these examples on figure 7.

5. Boundaries of existence domains for different solutions

In our studies of the bifurcation structure of PP and EE solutions, we encountered some special two-fluid flows which formed the boundaries of domains of existence. These are $P(k_1)C$, $CP(k_2)$ and $PE(k_1)PE(k_2)$. The first two solutions consist of periodic P and constant C velocity profiles, the third type is a $P(k_1)P(k_2)$ solution which is also symmetric with respect to reflection about the axis $\phi = 0$. Each solution of this type exists only in a set of codimension-one in the parameter space (R_1, R_2) (i.e. a curve or several curves). Another solution important for bifurcation structure is the CC solution, corresponding to the velocity in both fluids being constant. It is a matter of simple algebra to show that there are only two CC solutions: one with both fluids being motionless, another one with the velocity in each fluid being $\nu_1 U_{cc}/r$, where $U_{cc} = 4(\lambda - \delta)/(\delta - \lambda^2)$. The first case corresponds to the origin in the (R_1, R_2)-plane, the second case to a straight line $(R_1, R_2) = (U_{cc}\alpha, \lambda U_{cc}(2\pi - \alpha))$, since the angle α $(0 < \alpha < 2\pi)$ can now be chosen arbitrarily.

To understand how existence domains for different PP and EE solutions overlap, we plot several PC, CP and $PE\ PE$ solutions on figure 9. We see that the curves for many of these special solutions on the (R_1, R_2)-plane end at the origin $(R_1, R_2) = (0, 0)$, each having a finite angle with respect to the others. Examples of such solutions are $PE_1\ PE_1$, CP_1, CP_2, CP_3 (in fact, all $CP(k_2)$ and $P(k_1)C$ solutions we studied end at the origin in this way). We note that P_1C ends at the origin as well, as is evident from figure 5; however, P_1C is not shown on figure 9 to avoid overcrowding the origin. Note that the origin $(R_1, R_2) = (0, 0)$ is the trivial CC solution itself. For the cases we studied, the boundaries of the domain of existence of EE solutions contained PC and CP cases. Therefore, the boundary of the existence domain of a $E(k_1)E(k_2)$ solution contains two curves intersecting at the origin. On the other hand, most $PE(k_1)PE(k_2)$ solutions do not end at the origin, the exception being PE_1PE_1. It is also clear from figure 9 that increasing the indices k_1 and k_2 moves the curves $PE(k_1)PE(k_2)$ to the right, expanding the region of existence of $P(k_1)P(k_2)$ flows.

We should emphasize that we have only performed calculations with given values of parameters $\lambda = 1/2$ and $\delta = 1/8$. For other values of these parameters the geometry

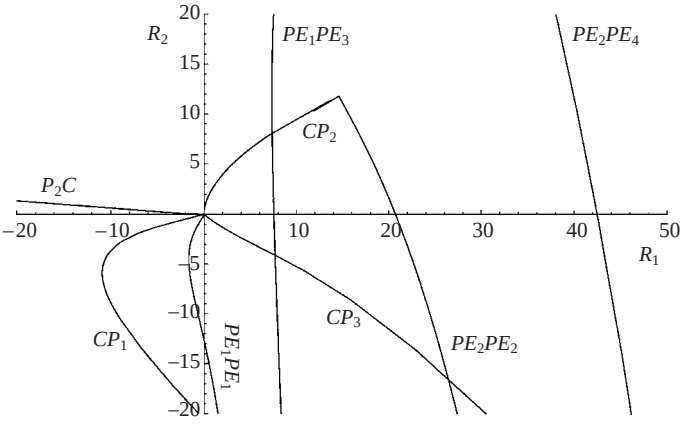

FIGURE 9. Several special solutions *PE PE*, *PC* and *CP* marking the boundaries of existence domains of *PP* and *EE* solutions.

of the domains of existence might change. However, the position of the existence domains for different solutions can always be obtained by analysing the positions of $PE(k_1)PE(k_2)$, $CP(k_2)$ and $P(k_1)C$ solutions on the (R_1, R_2)-plane.

6. Multiple stationary solutions and linear stability

It is interesting to discuss the number of possible solutions for specified values of R_1 and R_2. Both $P(k_1)P(k_2)$ and $E(k_1)E(k_2)$ solutions are defined in a large part of the parameter space. In addition, we observed numerically that increasing k_1 and k_2 will in general increase the domain of existence of solutions. Also, for the classical Jeffery–Hamel problem and the free-space generalization, infinitely many solutions exist. Based on this information, we formulate the following

CONJECTURE 1. *For each pair* (R_1, R_2) *there is an infinite number of solutions of types* $P(k_1)P(k_2)$ *and* $E(k_1)E(k_2)$ *with sufficiently large* k_1 *and* k_2.

The case of $SE(k_2)$ solutions is more complex. First, $SE(k_2)$ flows are defined only in a finite range of parameter values R_1, R_2. Second, $SE(k_2)$ solutions seem to exhibit exceedingly small values of angles α. Therefore, we do not know whether there is a finite or an infinite number of these solutions for given (R_1, R_2). Demonstrating that only a finite number (or none) of these solutions exist for some values of (R_1, R_2) will reveal another interesting feature of the two-fluid problem.

In view of the fact that for given R_1 and R_2 there are many solutions, the question of linear stability is crucial for deciding which solutions are chosen in nature. In this article, we have not discussed the linear stability of two-fluid solutions, which can only be analysed through extensive numerical simulations. However, the linear stability analysis alone seems to be insufficient for choosing the solution. Recent work on the stability of Jeffery–Hamel flows and their generalizations by Uribe *et al.* (1997), Eagles & Georgiou (1987), Eagles (1966), Goldshtik *et al.* (1991), Sobey & Drazin (1986), Dennis *et al.* (1997) and Shusser & Weihs (1995, 1996) distinguish two types of stability. *Spatial stability* concerns the development of stationary perturbations at large r. *Temporal stability* concerns the development of time-dependent perturbations. In the case of temporal stability, the linear stability analysis is performed in the annulus $r_0 \leqslant r \leqslant r_1$. The boundary conditions at the inner and outer radii are

difficult to derive physically, and different boundary conditions seem to affect the results greatly, as shown by Putkaradze & Romero (2003). Further understanding of the linear stability of the flow is needed, which will be the subject of future work. In addition, laboratory experiments would be very interesting and useful.

7. Conclusions

In this paper, we have discussed novel solutions describing planar stationary motion of two fluids from a point source. Except for the single-fluid case described in § 4, the bifurcations of solutions are not subcritical, which makes it plausible that the two-fluid solutions may be observed in an experiment. We have also presented a classification of all possible solutions. Our method is superior to Newton's method with continuation since not all solutions can be obtained by Newton's method.

The solutions we described admit an interesting generalization in three dimensions, describing three-dimensional flow of one fluid into another. This will lead to a two-fluid generalization of Squire–Wang flows, with velocities inversely proportional to the spherical radius, which we intend to address in future work. The theory of Squire–Wang flows has been an area of active research for many years, see Squire (1952), Wang (1991), Pillow & Paull (1985), Paull & Pillow (1985*a*, *b*), Goldshtik & Shtern (1990). Two-fluid generalizations of such flows would be very interesting from both academic and applied points of view.

The author acknowledges useful discussions with J. Deshler, T. Kapitula, L. Romero and P. Weidman. The support of A. Sallinger is acknowledged. This work was partially supported by a Sandia National Laboratory SURP grant.

Appendix. An algorithm for finding solutions of type $P(k_1)P(k_2)$

In order to clarify the way $P(k_1)P(k_2)$ solutions are computed, we present our algorithm as a series of steps. This will also elucidate the bifurcation structure of the solutions.

(*a*) *Choose two parameters* (α, τ_1) *or* (α, τ_2)

If one of the imaginary periods τ_j is chosen as a parameter, the other imaginary period must be computed from the normal stress boundary condition (2.4*c*) using the connection (2.5) between periods and invariants. We impose a condition on the choice of parameterization. If we choose (α, τ_1) as parameters, for example, we must be able to solve (2.4*c*) for $\tau_2(\alpha, \tau_1)$ for arbitrary values of τ_1. By studying the behaviour of the invariants a_j as the function of the periods, we conclude that the desired parameterization is

$$\left.\begin{array}{ll}(\alpha, \tau_1)\, \tau_2 = \tau_2(\alpha, \tau_1) & \text{when } \alpha < \alpha_c, \\ (\alpha, \tau_2)\, \tau_1 = \tau_1(\alpha, \tau_2) & \text{when } \alpha > \alpha_c, \end{array}\right\} \tag{A 1}$$

where α_c satisfies

$$\delta\left(\frac{4\pi^4 k_1^4}{\alpha_c^4} - 4\right) = \left(\frac{4\pi^4 k_2^4}{(2\pi - \alpha_c)^4} - 4\right). \tag{A 2}$$

For example, for the choice of parameters $\nu_1/\nu_2 = \lambda = 0.5$, $\rho_1/\rho_2 = 0.5$, $k_1 = 1$, $k_2 = 3$ which we use in calculations, (A 2) yields $\alpha_c \simeq 1.05818 \simeq 0.336829\pi$.

(*b*) *Compute second imaginary period from* (2.4*c*)

The choice of parameterization (A 1) ensures that this is always possible. In this step, we know α, τ_1, τ_2 together with real periods $p_1 = \alpha/k_1$, $p_2 = (2\pi - \alpha)/k_2$.

(*c*) *Determine the values of the functions* $f_j(\phi)$ *at* $\phi = -\alpha/2$

Square the second equation of (2.4*b*) and use (2.3) to obtain

$$\left.\begin{aligned} &\lambda(6f_1 + 2) = 6f_2 + 2, \\ &\delta^2\left(4f_1^3 - a_1 f_1 - b_1\right) = 4f_2^3 - a_2 f_2 - b_2, \end{aligned}\right\} \tag{A 3}$$

where we denoted for simplicity $f_j = f_j(-\alpha/2)$. System (A 3) defines a cubic equation for each f_1 and f_2 which has either one or three real roots. After the solution is computed, however, we must check the sign of the derivative of f_i at $\phi = \alpha/2$ to ensure that (2.4*b*) is satisfied with the correct sign, because second equation of (2.4*b*) was squared.

(*d*) *Find the phase shifts* θ_j

Once a real solution f_1, f_2 of (A 3) is found, we can obtain θ_j from the formula

$$f_j = \mathscr{P}(\mathrm{i}\tau_j + \theta_j, \{p_j, 2\mathrm{i}\tau_j\}), \tag{A 4}$$

with $p_1 = \alpha/k_1$, $p_2 = (2\pi - \alpha)/k_2$. The function on the right-hand side of (A 3) as a function of θ oscillates between $f_{j,min}$ and $f_{j,max}$. Therefore, for (A 4) to be solvable, we need to make sure that $f_{j,min} \leqslant f_j \leqslant f_{j,max}$.

(*e*) *Compute* R_1 *and* R_2

When θ_j are found, we can determine R_1 and R_2 using the flux condition (2.4*d*). In the case of $P(k_1)P(k_2)$ solutions, the flux condition can be calculated exactly in terms of Weierstrass Zeta Functions ζ, see Chandrasecharan (1984):

$$\left.\begin{aligned} R_1 &= \lambda\left(12k_1\zeta\left(\frac{\alpha}{2k_1}; a_1, b_1\right) - 2\alpha\right), \\ R_2 &= 12k_2\zeta\left(\frac{2\pi - \alpha}{2k_2}; a_2, b_2\right) - 2(2\pi - \alpha). \end{aligned}\right\} \tag{A 5}$$

The algorithm is completed and the desired $P(k_1)P(k_2)$ solution is obtained. For each $P(k_1)P(k_2)$ solution, a mirror image about $\phi = 0$ is also a solution. Using the parameterization (τ_j, α) instead of (R_1, R_2), we have avoided the necessity to invert the mapping between these two parameters defined by (A 5). We discovered that this mapping is two-to-one for some values of parameters so our way of parameterization of the solution is preferable.

REFERENCES

Banks, W. H. H., Drazin, P. G. & Zaturska, M. A. 1988 On perturbations of Jeffery–Hamel flow *J. Fluid Mech.* **186**, 559–581.

Berker, R. 1963 *Handbuch Der Physik*, VIII/2, pp. 20–23. Springer.

Bourgin, P. & Tahiri, N. 1995 Generalized Jeffery–Hamel flow: application to high velocity coating, In *Proc. First European Coating Symp., University of Leeds* (ed. P. H. Gaskell, M. D. Savage & J. L. Summers), pp. 23–31.

Chandrasecharan, K. 1984 *Elliptic Functions.* Springer.

Dennis, S. C. R., Banks, W. H. H., Drazin, P. G. & Zaturska, M. B. 1997 Flow along a diverging channel. *J. Fluid Mech.* **336**, 183–202.

Eagles, P. M. 1966 The stability of a family of Jeffery–Hamel solutions for divergent channel flow. *J. Fluid Mech.* **24**, 191–207.

Eagles, P. M. & Georgiou, G. A. 1987 Evolution of some isolated disturbances to Jeffery–Hamel flow. *Phys. Fluids* **30**, 3838–3840.

Fraenkel, L. E. 1962 Laminar flow in symmetrical channels with slightly curved walls. I. On the Jeffery–Hamel solutions for the flow between plane walls. *Proc. R. Soc. Lond.* A **267**, 119–138.

Fraenkel, L. E. 1963 Laminar flow in symmetrical channels with slightly curved walls. II. An asymptotic series for the stream function *Proc. R. Soc. Lond.* A **272**, 406–428.

Georgiou, G. A. & Eagles, P. M. 1988 The stability of flows in channels with small wall curvature. *J. Fluid Mech.* **14**, 259–287.

Goldshtik, M. A., Hussain, F. & Shtern, V. N. 1991 Symmetry breaking in vortex-source and Jeffery–Hamel flows. *J. Fluid Mech.* **232**, 521–566.

Goldshtik, M. A. & Shtern, V. N. 1989 Loss of symmetry in viscous flow from a linear source. *Fluid Dyn.* **24**, 191–199.

Goldshtik, M. & Shtern, V. 1990 Collapse in conical viscous flows. *J. Fluid Mech.* **218**, 483–508.

Hamel, G. 1916 Spiralförmige Bewegungen zäher Flüssigkeiten. *Jahresbericht Deutsch. Math. Verein* **25**, 34–60.

Jeffery, G. B. 1915 The two-dimensional steady motion of a viscous fluid. *Phil. Mag.* (6) **29**, 455–465.

Landau, L. D. & Lifshitz, E. M. 1987 *Fluid Mechanics*. Pergamon.

Moffatt, H. K. & Duffy, B. R. 1980 Local similarity solutions and their limitations. *J. Fluid Mech.* **96**, 299–313.

Paull, R. & Pillow, A. F. 1985*a* Conically similar viscous flows. Part 2. *J. Fluid Mech.* **155**, 343–358.

Paull, R. & Pillow, A. F. 1985*b* Conically similar viscous flows. Part 3. *J. Fluid Mech.* **155**, 359–379.

Pillow, A. F. & Paull, R. 1985 Conically similar viscous flows. Part 1. *J. Fluid Mech.* **155**, 327–341.

Putkaradze, V. & Dimon, P. 2000 Nonuniform two-dimensional fluid flow from a point source. *Phys. Fluids* **12**, 66–70.

Putkaradze, V. & Romero, L. 2003 Stability of two-dimensional flows from a point source. *J. Fluid Mech.* (submitted).

Rosenhead, L. 1940 The steady two-dimensional radial flow of viscous fluid between two inclined plane walls. *Proc. R. Soc. Lond.* A **175**, 436–467.

Shusser, M. & Weihs, D. 1995 Stability analysis of source and sink flows. *Phys. Fluids* **7**, 2345–2354.

Shusser, M. & Weihs, D. 1996 Stability of source-vortex and doublet flows. *Phys. Fluids* **8**, 3197–3199.

Sobey, I. J. & Drazin, P. G. 1986 Bifurcations of two-dimensional channel flows. *J. Fluid Mech.* **171**, 263–287.

Squire, B. 1952 Some viscous flow problems. *Phil. Mag.* **43**, 942–945.

Thom, R. 1975 *Structural Stability and Morphogenesis*, p. 92. Benjamin.

Uribe, F. J., Diaz-Herrera, E., Bravo, A. & Peralta-Fabi, R. 1997 On the stability of the Jeffery–Hamel flow. *Phys. Fluids* **9**, 2798–2800.

Voropayev, S. I. & Afanasyev, Ya, D. 1992 Two-dimensional vortex dipole interactions in a stratified fluid. *J. Fluid Mech.* **236**, 665–689.

Voropayev, S. I. & Afanasyev, Ya, D. 1994 Symmetric interaction of developing horizontal jet in a stratified fluid with vertical cylinder. *Phys. Fluids* A **6**, 2032–2037.

Voropayev, S. I. & Fernando, H. J. S. 1996 Propagation of grid turbulence in homogeneous fluids. *Phys. Fluids* **8**, 2435–2440.

Voropayev, S. I., Fernando, H. J. S. & Wu, P. C. 1996 Steady and unsteady quadrupolar flow. *Phys. Fluids* **8**, 384–396.

Wang, C. Y. 1991 Exact solutions of steady-state Navier–Stokes equations. *Annu. Rev. Fluid Mech.* **23**, 159–177.